

Modelling Accidental Industrial liquid petroleum gas (LPG) Releases with PHOENICS two phases IPSA algorithm

Jean-Marc Lacomme¹, Jalil Ouazzani², Patrick Bonnet¹ and Yves Dagba¹

¹ Ineris, Parc Technologique Alata 60550 Verneuil en Halatte, France

² Arcofluid, Parc Innolin, 3 Rue du Golf, 33700 Mérignac, France

ABSTRACT

INERIS has been involved in a European project called FLIE (Flashing Liquids in Industrial Environment). In the scope of this project, INERIS carried out large-scale experiments with propane and butane releases on the experimental set-up at the INERIS test site. INERIS researchers were having also as objective to develop models of flashing releases as encountered in realistic industrial environments. Equivalent source term models exist for flashing release in current long-range dispersion models. Several factors can, however, invalidate simplified equivalent source models, especially in the very near field where obstacles can be found. Therefore one has to resort to full 3D numerical modelling of the transport equations.

The numerical modelling consists in using the Phoenix CFD code in order to simulate the releases of liquid butane in the atmosphere, with and without the presence of an obstacle. The used technique of two phases atmospheric dispersion is a Eulerian - Eulerian approach based on the IPSA method. The inlet boundary conditions for this CFD modelling are based on experimental data: mass release, droplet velocity and mean droplet size within the jet. To handle evaporation from puddle pools, specific boundary conditions were introduced.

Two experimental cases of butane releases, a free jet and an impinging jet on a blockage have been chosen in order to perform the numerical simulations. We have then compared the calculated results with the experimental measurements taken within the jet and from the pools formed by LPG releases. The characteristics of the two studied cases were identical except that in the case of the impinging jet there is a wall located at two meters from the release point. Up to now, few CFD modelling of flashing jets in industrial environments, were realised with data experimental inputs.

The average global behaviours of the free jet and impinging jet are well represented by simulations. The evolutions of the calculated temperatures within the jet are compared with the experimental data. The quantitative estimate of the evaporation within the jet and also from the puddle pools are compared with the experimental data in the case of the free jet (not impinging) and the impinging jet. The validation of this CFD modelling will allow improving the estimate of an equivalent source term for far field atmospheric dispersion calculations in realistic industrial environments.

1. INTRODUCTION

INERIS has started a research program to understand and develop in-house the theoretical and experimental approaches in LPG problems. One of the task was to customize the Phoenix software to be used within the framework of problem of industrial risks concerning the leakages of pollutant or dangerous gas in the form of droplets (evaporating then in the ambient air), and of vapour possibly. Based on an experimental model developed at INERIS on a controlled leakage in ambient air, a theoretical and numerical approach using the Phoenix code has been overtaken, where for the numerical aspect ArcoFluid has been involved. Two techniques available in Phoenix were used to treat this kind of problems, the IPSA (1) technique which is an Eulerian approach and the GENTRA (2) technique which is a Lagrangian approach. In these two methods, the exchanges of mass, moment and energy are considered. The IPSA algorithm uses a continuous formulation of the equations for the two phases in such way that gases and particles are treated as mediums which interpenetrate.

In the Lagrangian approach, the movement and the transport of samples representative of discrete particles are followed in the field of the flow by using a set of ordinary differential equations coupled to the partial differential equations of the transport equations of the carrier fluid solved through an Eulerian method.

Even if in this paper both methods have been used, we will focus only on the IPSA algorithm used to setup the physical problem under consideration which is described below.

2. DESCRIPTION OF THE PROBLEM

The experiments which have been done at INERIS consisted of sending a jet of liquid butane or propane in the atmosphere. The jet is coming out from a standing stud with a circular hole. The stud is connected to an external reservoir of Butane or propane, and is located under a cabin with no lateral walls and a removable frontal wall. The experiments can be performed with (impinging jet) or without the front wall (free jet). In order to collect temperature data's, several thermistors are placed all around the stud and it's vicinity, faraway and also behind. A fast recording camera is placed in such a manner that one can visualise the aerosol movement.

We have therefore treated numerically with the IPSA algorithm two classes of cases. One class corresponds to the free jet and the other to the impinging jet. Furthermore we have introduced a source term in the equation's to be able to handle the evaporation from the surface.

In order to follow the size of the droplet we have used the shadow method included in the IPSA algorithm of Phoenics which consists of solving a third phase without mass transfer.



Fig 1 Surrounding of the experimental setup. Inside the cabin is vertical stud connected to the Butane (propane) tank from where a jet is coming to the ambient air. The blue wall is removed for the free jet case.

Two experimental cases of butane releases, a free jet and an impinging jet on a wall blockage have been chosen in order to perform the numerical simulations. We have then compared the calculated results with the experimental measurements taken within the jet and from the pools formed by LPG releases.

3. GENERAL EQUATIONS

The presence of droplets and gas in each cell of control is represented in PHOENICS through local volume fractions r_1 and r_2 . These two quantities obey the same differential equations that the other quantities and take part in all the differential equations:

For a gas mixture of air-butane :

$$\frac{\partial \rho_1 r_1}{\partial t} + \text{div}(\rho_1 r_1 \mathbf{V}_1^\rho) = m_p \quad (1)$$

$$\frac{\partial \rho_1 r_1 \mathbf{V}_1^\nu}{\partial t} + \text{div}(\rho_1 r_1 \mathbf{V}_1^\rho \mathbf{V}_1^\rho) = -r_1 \text{grad}(P_1) + \text{div}(\Gamma_{\mathbf{V}_1^\rho} r_1 \nabla \mathbf{V}_1^\rho) + r_1 \rho_1 \mathbf{g} + \mathcal{S}_{ip}^\rho \quad (2)$$

$$\frac{\partial \rho_1 r_1 H_1}{\partial t} + \text{div}(\rho_1 r_1 \mathbf{V}_1^\rho H_1) = \text{div}(\Gamma_{H_1} r_1 \nabla H_1) + S_{H_1} + H_{ip1} \quad (3)$$

$$\frac{\partial \rho_1 r_1 W_1}{\partial t} + \text{div}(\rho_1 r_1 \mathbf{V}_1^\rho W_1) = \text{div}(\Gamma_{W_1} r_1 \nabla W_1) + m_p \quad (4)$$

For butane droplets:

$$\frac{\partial \rho_2 r_2}{\partial t} + \text{div}(\rho_2 r_2 \mathbf{V}_2^\rho) = -m_p \quad (5)$$

$$\frac{\partial \rho_2 r_2 \mathbf{V}_2^\nu}{\partial t} + \text{div}(\rho_2 r_2 \mathbf{V}_2^\rho \mathbf{V}_2^\rho) = -r_2 \text{grad}(P_1) + \text{div}(\Gamma_{\mathbf{V}_2^\rho} r_2 \nabla \mathbf{V}_2^\rho) + r_2 \rho_2 \mathbf{g} - \mathcal{S}_{ip}^\rho \quad (6)$$

$$\frac{\partial \rho_2 r_2 H_2}{\partial t} + \text{div}(\rho_2 r_2 \mathbf{V}_2^\rho H_2) = \text{div}(\Gamma_{H_2} r_2 \nabla H_2) + S_{H_2} + H_{ip2} \quad (7)$$

These equations are similar to the monophasic equations except for the introduction of the volume fractions r_1 and r_2 , and of the sources terms related to inter phase exchange which are m_p (mass exchanged between the liquid and the gas-vapour mixture), \mathcal{S}_{ip}^ν source of inter phase transfer of momentum, H_{ip} source of inter phase transfer of energy (1-6). The Γ_i are the laminar and turbulent coefficients of diffusion for each variable. Indices 1 and 2 represent phase 1 and phase 2. With these equations, one can associate the model of turbulence of his choice. (In general, the model K - ϵ is the selected model, and it was the choice in this work). For r_1 and r_2 , they must obey the following constitutive relation:

$$\mathbf{r}_1 + \mathbf{r}_2 = \mathbf{1} \quad (8)$$

Some authors (4,5) recommend that with the small diameters of the butane droplets, one can suppose that a fast balance towards saturation is done in such way that it is not necessary to solve equation (7) but instead to take saturation temperature relations. That is not the case here, and equation (7) is solved. The transfer of heat between the droplets and the air mixture - vapour is modelled in this case by a heat flow (per unit of volume):

$$q_{avp} = -h^* (T_{gaz} - T_{gout}) * \frac{6r_2}{d} \quad (9)$$

With the coefficient h given by the correlation of Frossling :

$$h = \lambda_m * \frac{\left(2.0 + 0.75 * Re^{\frac{1}{2}} Pr^{\frac{1}{3}}\right)}{d} \quad (10)$$

λ_m thermo conductivity of binary mixture air-vapour
 Re Reynolds number based on slip inter phase velocity
 Pr Prandtl number based on the properties of the mixture
 D Droplets diameter
 T_{gout} Droplets temperature
 T_{gas} Mixture temperature

The term of source of mass m_p (kg/m³/s) which results from it, is:

$$m_p = h * (T_{gaz} - T_{satp}) * \frac{6r_2}{d} * \frac{1}{L_p} \quad (11)$$

L_p Latent heat of vaporization
 T_{satp} vapour saturation temperature

which enables us to define H_{ip1} :

$$H_{ip1} = \left[h * \frac{6r_2}{d * Cp_m} + \max(0, m_p) \right] * (Cp_m * T_{gout} - H_1) \quad (12)$$

Cp_m Mixture Specific heat

And, also H_{ip2} :

$$H_{ip2} = \left[h * \frac{6r_2}{d * Cp_{liq}} \right] * (Cp_{liq} * T_{gaz} - H_2) \quad (13)$$

Cp_{liq} Droplets specific heat

With regard to the source term of interfacial transfer of momentum $\overset{p}{S}_{ip}$:

It is calculated automatically by PHOENICS by taking the option “dispersed fluid drag models”. This option corresponds to CFIPS=GRND7 and is equivalent to:

$$\overset{p}{S}_{ip} = C_D * r_2 * \rho_1 * |V_1^p - V_2^p| * \frac{(V_1^p - V_2^p)}{d} \quad (14)$$

With the coefficient CD calculated as follow:

$$CD = \left[\frac{24}{Re} \right] (1 + 0.15 * Re^{0.687}) + \left[\frac{0.42}{1.0 + 4.25 * 10^4 Re^{-1.16}} \right]$$

Besides the source S_{ip}^P , the other sources are calculated by the user after deactivating the default source terms of Phoenix.

To be able to take into account the change of size of the droplets due to evaporation, one associates with these equations an additional equation for the quantity r_s , the shadow volume fraction of phase 2. This equation is the same one as for r_2 (eq. 5) except that it does not have a source term of mass transfer. Once obtained r_2 and r_s , one can deduce the new size of the droplets from:

$$\frac{d}{d_0} = \left(\frac{r_2}{r_s} \right)^{\frac{1}{3}} \quad (15)$$

Where d_0 is the initial diameter. This change is then reflected on the interphases laws.

4. LAWS FOR THE GAS-VAPOUR MIXTURE

To take into account the air - vapour mixture (that it is in IPSA or GENTRA), one has to calculate the physical properties of the mixture which will be mainly useful for laminar regions. We do these calculations in ground.for by using the following mixture laws:

Dynamic viscosity:

$$\mu_m = \frac{\sum_{i=1}^n x_i \mu_i}{\sum_{j=1}^n x_j \phi_{ij}} \quad (16)$$

$$\phi_{ij} = \frac{1}{\sqrt{8}} \left(1 + \frac{M_i}{M_j} \right)^{\frac{1}{2}} \left[1 + \left(\frac{\mu_i}{\mu_j} \right)^{\frac{1}{2}} \left(\frac{M_j}{M_i} \right)^{\frac{1}{4}} \right]^2 \quad (17)$$

This formula gives us μ_m in $\text{gcm}^{-1}\text{s}^{-1}$.

Thermal conductivity:

$$\lambda_m = \frac{\sum_{i=1}^n x_i \lambda_i}{\sum_{j=1}^n x_j \phi_{ij}} \quad (18)$$

This formula gives us λ_m in $\text{cal cm}^{-1} \text{s}^{-1} \text{K}^{-1}$.

Specific heat:

$$Cp_m = \sum_{i=1}^n W_i Cp_i \quad (19)$$

With the molar fraction x_i obtained from the calculated mass fractions W_i :

$$x_i = \frac{\frac{W_i}{M_i}}{\sum_{j=1}^n \frac{W_j}{M_j}} \quad (20)$$

Binary diffusion coefficient (obtained from critical values of each component):

$$D_{AB} = a \left(\frac{T}{\sqrt{T_{CA} T_{CB}}} \right)^b * \frac{(P_{CA} P_{CB})^{\frac{1}{2}}}{P} * (T_{CA} T_{CB})^{\frac{5}{12}} * \left(\frac{1}{M_A} + \frac{1}{M_B} \right)^{\frac{1}{2}} \quad (21)$$

$$a = 2.74510^{-4}$$

$$b = 1.823$$

D_{AB} (cm²/s), T(K), P(atm).

5. BOUNDARY CONDITIONS

For all the cases, the external field will be considered has having a log type profile.

This profile is written like:

$$U = \frac{U^*}{k} \log \left(\frac{z}{z_0} \right) \quad (22)$$

$$k=0.4, z_0 = h_s/10 \text{ m}, h_s = 210^{-2} \text{ m}.$$

A 45 ° angle wind is entering the domain by faces “LOW” and “WEST” with an amplitude of 0.7m/s and an average temperature of 15°C. Faces “HIGH” and “EAST” of the field are considered as exits. The total size of the field is 18m X 6m X 18m in X, Y and Z respectively, Y represents the vertical variation, X the side variation and Z the axial variation according to the direction of the jet.

The solid stud of size (0.2 m X 1.5m X 0.2 m) is positioned in the field with the position x= 4.4m, y=0m and z= 3.8m.

This stud is surrounded by top, back and front walls of 9m² each one. In the case of the impinging jet (Fig. 1), the front wall is removed..

A fluid flush butane in the form of droplets is coming out at a rate of 0.9kg/s from an opening of diameter 10mm located on the high face of the stud. The centre of the hole is at the following position (x=4.41m, y=1.25m and z=4m). The diameter of the droplets is 10⁻⁰⁴m.

With these parameters, the incoming liquid jet enter the domain at a speed of 20m/s and a temperature of -45°C.

6. SURFACE EVAPORATION TREATMENT

Not being able to distinguish a distinct frontier between the puddle surface and the bulk, we have chosen to represent the evaporation from the surface of the puddle by considering a volumetric source approach which consists of calculating a surface evaporation from each cell which are below a specified height using the semi-empirical following relations:

$$q_v = q''_v * \frac{Vol}{\Delta l} * r_2$$

$$q''_v = k_m * P_{satv} * \frac{M_v}{RT_{liq}} \quad (23)$$

$$k_m = C_{m\&m} * \bar{u} * (2 * \Delta l)^{-0.11} * Sc^{-0.67}$$

$$C_{m\&m} = 0.004786$$

$$\bar{u} = \sqrt{u^2 + v^2}$$

$$\Delta l = \sqrt{dx^2 + dy^2 + dz^2}$$

With

A	Cell area (dx*dz)
Sc	Schmidt number
P _{satv}	Saturated Vapour pressure
T _{liq}	Liquid temperature in the cell
Vol	Cell volume dx*dy*dz

7. RESULTS

In fig. 2, we have plotted the total evaporated mass versus time for both cases, the free jet case as well as the impinging one. The simulation was performed for a 120 s.

We have also plotted in the same figure the part due to the surface evaporation in both cases. We can see that the evaporation follows the same trend for both cases in quite a linear manner but with a little bit more evaporation in the case of the impinging jet. This is mainly due to the fact that with the impact wall we have more turbulent dispersion and a larger surface of the broken jet in the ambient air.

Similarly, the evaporation at the surface is higher for the impinging case but is much lower than the bulk evaporation.

The impinging jet generates an important return of the liquid towards the back of the field and disperses more droplets in the vicinity of the impact. One can notice that there is a cooling of the air to the back of the stud in the case of the jet impinging at contrast to the free jet case.

The temperature was plotted in figure 3 and 4 at different locations in space designed per TH. These locations correspond to the experimental locations of the experimental thermistors. The value and the behaviour of the temperature at these points is analogous to the experimental results. These comparisons will be made in a coming publication.

We can see from figure 6a and 6b which represent respectively, iso-surfaces and iso-contours of temperature in the case of the impinging jet how the jet is cooling in the back of the stud and around the frontal blocking wall. Whereas in the free jet of similar figures (7a and 7b), the cooling is mainly in the front surface away from the stud, with little influence in terms of temperature field on the back of the stud.

Fig 7a shows the jet behaviour in the case of the free jet by the representation of the volume fraction of the liquid phase, and similarly by visualising the velocity module in the case of the impinging jet we have an image of the flow pattern as seen in fig 7b.

8. CONCLUSION

This work has permitted to demonstrate the ability of the Phoenix software to handle an LPG problem considering a binary mixture of air-butane and a liquid jet of butane.

The average global behaviours of the free jet and impinging jet are well represented by the simulations. The evolutions of the calculated temperatures within the jet are compared satisfactorily with the experimental data. The validation of this CFD modelling allow us improving the estimate of an equivalent source term for far field atmospheric dispersion calculations in realistic industrial environments. This work is still under investigation and will be developed further.

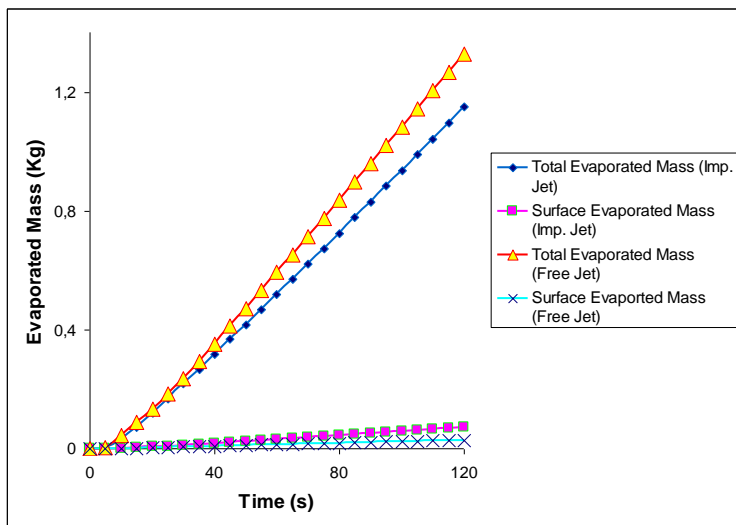


Figure 2: Comparison in the time of the total evaporated masses and surface in both cases of jet (impacting and free)

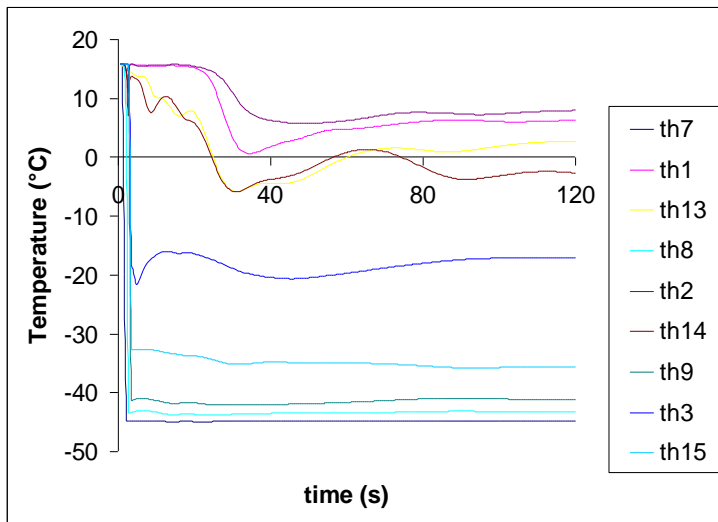


Figure 3: Followed by the change of the temperature in points gauges of the field in the case of the impacting jet, these points are as follows:

Position of the points TH (X, y, Z) compared to the source of emission of the liquified gas, these points are taken by considering the center of the opening of injection to the position (0,0,0):

TH1(0, 0.15, 0.47); TH2(0, 0.23, 0.98); TH3(0, 0.34, 1.92); TH7(0, 0, 0.47); TH8(0, 0, 0.98); TH9(0, 0, 1.92); TH13(0, -0.12, 0.47); TH14(0, -0.21, 0.99); TH15(0, -0.32, 1.92)

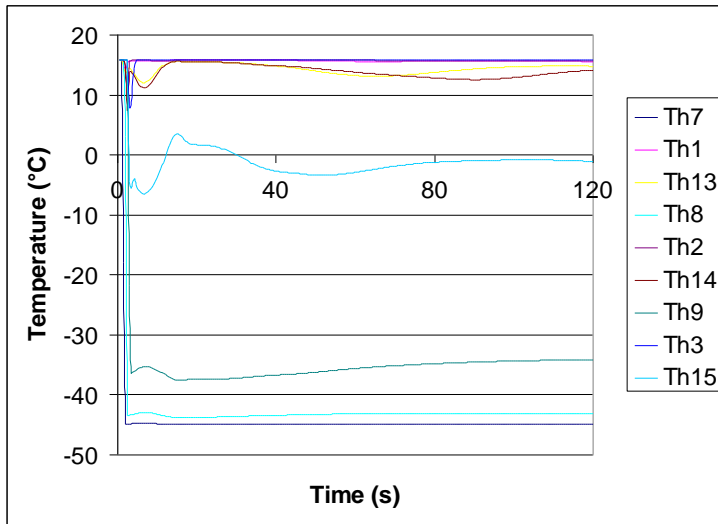


Figure 4: Follow-up of the change of the temperature in points gauges of the field in the case of the free jet (definition of the identical points that in figure 2).

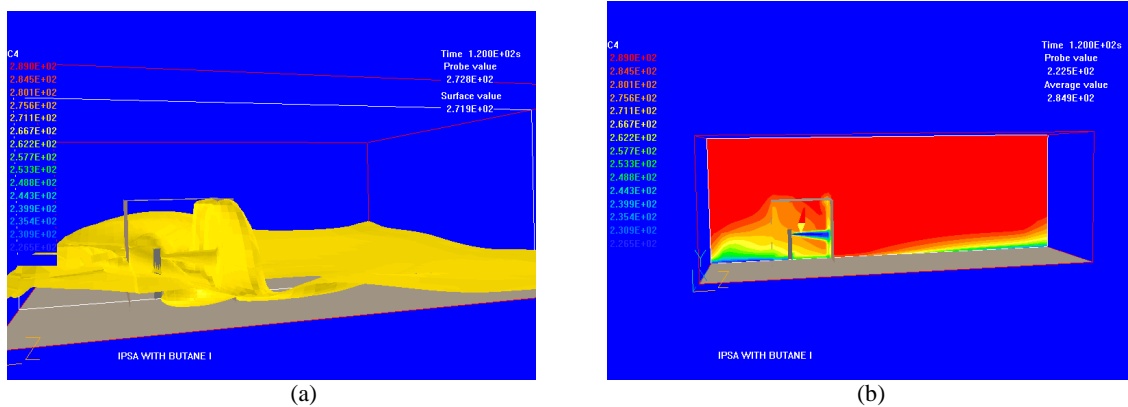


Figure 5a: Iso surfaces (271.19K) average temperature of cell with 120s in the case of the impacting jet, Figure 5b: Iso contours of the temperature in a plan passing by the medium of the opening of the free jet at time 120s.

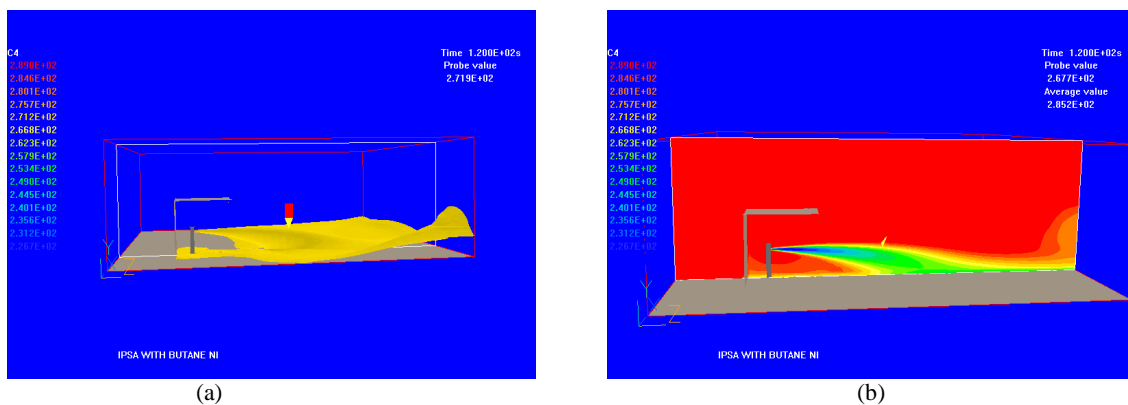


Figure 6a: Iso surfaces (271.19K) average temperature of cell with 120s in the case of the free jet, Figure 6b: Iso contours of the temperature in a plan passing by the medium of the opening of the jet impacting at time 120s.

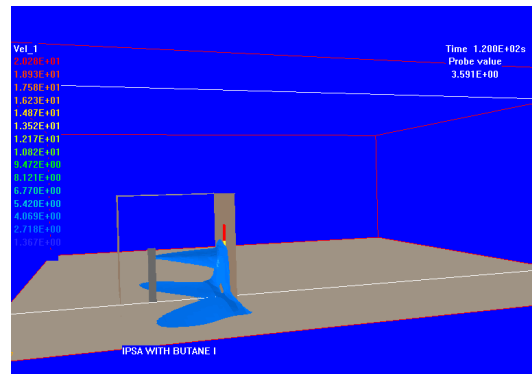
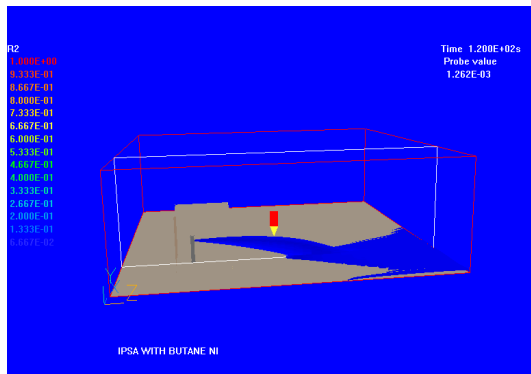


Figure 7a: Iso surfaces (1.262×10^{-3}) of the volume fraction r_2 , at time 120s in the case of the free jet, Figure 7b: Iso surfaces (3.591m/s) of the velocity module for phase 1 at 120s in the case of the impacting jet.

9. References

- [1] P.K. Hedberg, H.I. Rosten, D.B. Spalding: The Phoenix Equations – CHAM TR/99 – 1986
- [2] J. Moffat, M.R. Malin: A user’s guide to “Gentra” , A general particle tracking program” - CHAM TR/211b – 1989
- [3] F. Durst, D. Milojevic, B. Schonung : Eulerian and lagrangian predictions of particulate two-phase flows: a numerical study – Appl. Math. Modelling, 1984, Vol 8, pp 101-115
- [4] S. Vandroux-Koenig, G. Berthoud : Modelling of a two phase momentum jet close to the breach, in the containment vessel of a liquefied gas – J. Loss Prev. process Ind. Vol 10. N° 1. pp. 17 – 29 , 1997
- [5] R.Schmehl, G.Klose, G.Maier, S.Wittig: Efficient Numerical Calculation of Evaporating Sprays in Combustion Chamber Flows, RTO-MP-14, presented at the 92nd Symp. on Gas Turbine Combustion, Emissions and Alternative Fuels, Lisbon, Portugal, 12-16 October 1998.
- [6] S. Wittig, M. Hallmann, M. Scheurlen, R. Schmehl: A New Eulerian Model for Turbulent Evaporating Sprays in Recirculating Flows, AGARD-CP-536, presented at the AGARD Conference on Fuels and Combustion Technology for Advanced Aircraft Engines, Fiuggi, Italy, 1993.